

## Adsorption of Unsaturated Hydrocarbons on Pd(111) and Pt(111): A DFT Study

Florian Mittendorfer,<sup>†</sup> C. Thomazeau,<sup>‡</sup> P. Raybaud,<sup>\*,‡</sup> and H. Toulhoat<sup>§</sup>*Division Chimie et Physico-chimie appliquées, Division Catalyse et Séparation, and Direction Scientifique, Institut Français du Pétrole, 1-4 avenue de Bois Préau – 92500 Reuil-Malmaison, Cedex, France**Received: June 11, 2003; In Final Form: September 1, 2003*

The adsorption of unsaturated hydrocarbons on metallic surfaces is of fundamental and applied interest, in view of its implications as a model system for catalysis in the refining industry. In particular, the relation between the type of hydrocarbon and its adsorption strength on metallic surfaces remains an open question. Thus, we propose a comparative DFT study of the adsorption of several relevant hydrocarbons on the catalytically relevant Pd(111) and Pt(111) surfaces. The key adsorption features (structural, electronic, energetic, and spectroscopic) are analyzed in a consistent way for two olefins (ethylene, 1-butene), one aromatic (benzene), one alkyne (acetylene), and one diolefin (1,3-butadiene). Whereas ethylene and 1-butene are adsorbed in a di- $\sigma$  mode, the flat adsorption of benzene takes place in a bridge position. For acetylene, the adsorption occurs in a 3-fold hollow site, whereas 1,3-butadiene adsorbs in a tetra- $\sigma$  configuration whatever the coverage. In the latter case, a vibrational analysis of the adsorption modes is proposed and compared to available HREELS data. A thermodynamic model, giving the variation of the Gibbs free energy of adsorption, enables a ranking of the relative stability of the adsorbates as a function of pressure and temperature. Finally, we suggest that the more selective hydrogenation of diolefins observed for Pd may be attributed to the lower adsorption strength of 1-butene on Pd, preventing its further hydrogenation into butane.

## 1. Introduction

The hydrogenation of hydrocarbons is a fundamental process in the chemical industry.<sup>1</sup> Sabatier discovered at the beginning of the 20th century that metal catalysts are able to activate the hydrogenation of double and triple bonds. Since then, a large number of studies have been performed to investigate this field, with the goal of gaining a detailed understanding of the catalytic activity of selected metals. Especially for reactions of a Langmuir–Hinshelwood-type mechanism, the chemisorption of the reactants on the surface constitutes a critical step.

Cosyns<sup>2</sup> proposed a volcano-shaped correlation between the adsorption of several families of hydrocarbons and corresponding catalytic activity. In this model, the aromatics would represent the family with the weakest adsorption corresponding to the weakest activity of a given noble metal, followed by increased activity for the olefins and the diolefins, and again weaker activity for the hydrogenation of acetylene. Two metallic systems, Pd and Pt, have been the focus of most studies because they play a great role in heterogeneous catalysis devoted to hydrogenation<sup>1</sup>. The developments in the field of computational chemistry, in the last few years, have made the investigations of realistic catalytic systems with a theoretical approach feasible. Thus, the adsorption of representative molecules, such as ethylene, on Pd or Pt surfaces has been covered with a large range of experimental techniques (such as LEED, EELS, STM, or TPD)<sup>3–10</sup> as well as theoretical approaches.<sup>11–13</sup> This is also the case for acetylene.<sup>8,12,14–20</sup> At the same time, benzene adsorption has also been the subject of many experimental investigations.<sup>8,17,21–26</sup> Recent DFT studies have also been devoted to benzene adsorption.<sup>27–29</sup> However, the adsorption

of diolefins such as butadiene has been investigated to a much lesser degree. Even if EELS,<sup>30</sup> HREELS, and NEXAFS<sup>31</sup> characterizations brought many insights on the adsorption of benzene on Pd(111) and Pt(111) surfaces, key questions about adsorption modes and strengths remain open. Only a few theoretical studies<sup>32</sup> have been devoted to this topic until now, and to our knowledge, no modern DFT simulation has been undertaken, although butadiene adsorption on Pd and Pt remains a crucial step for understanding the selective hydrogenation of diolefins.<sup>33–35</sup>

Thus, the present work will first determine the adsorption modes of butadiene on Pd(111) and Pt(111) by DFT calculations and by taking into account coverage effects. Then, regarding catalytic properties (activity as well as selectivity), it is of high interest to investigate the competitive adsorption on Pd(111) and Pt(111) for the above-mentioned unsaturated hydrocarbons. We will attempt to establish, in a consistent way, the order for the adsorption strength of the different hydrocarbons. The effects of temperature and pressure on this order will be addressed with the help of thermodynamic considerations. The main goal is to put forward general concepts governing the adsorption steps for those unsaturated hydrocarbons and simultaneously to compare the two metallic surfaces.

The adsorption of olefins will be represented by the adsorption of ethylene and 1-butene, and the adsorption of aromatics will be represented by the adsorption of benzene. The adsorption of acetylene will offer insights into the interaction of molecules with a triple bond with the metallic surface. A consistent and systematic comparison based on the electronic and energetic properties will be given for all species. In the case of the adsorption of butadiene, the investigation will be enriched by a vibrational analysis in order to clarify the adsorption modes.

This study will be presented as follows: section 2 will give an overview of the methodology used, and section 3 will be devoted to an investigation of the adsorption properties of the

\* Corresponding author. E-mail. pascal.raybaud@ifp.fr. Tel: +33 1 47 52 71 84. Fax: +33 1 47 52 70 58.

<sup>†</sup> Division Chimie et Physico-chimie appliquées.

<sup>‡</sup> Division Catalyse et Séparation.

<sup>§</sup> Direction Scientifique.

selected adsorbates, including the energetic and electronic properties at 0 K. In section 4, a thermodynamic model allowing the comparison of the adsorbed molecules as a function of  $T$  and  $P$  will be presented. Finally, conclusions will be drawn in section 5.

## 2. Methodology

All adsorption energies as well as electronic and vibrational properties are calculated by using the Vienna ab initio simulations package (VASP).<sup>36,37</sup> VASP performs an iterative solution of the Kohn–Sham equations of density functional theory (DFT). It is based on a plane wave basis set and uses the projector augmented wave (PAW) method<sup>38,39</sup> for the description of the electron–ion interactions. In addition, Perdew–Wang-91 (PW91) gradient corrections<sup>40</sup> have been used for the exchange–correlation functional. For the plane wave basis set, a cutoff of  $E_{\text{cut}} = 400$  eV has been used. The Brillouin-zone integration has been performed with a  $7 \times 7 \times 1$  Monkhorst–Pack grid<sup>41</sup> and a Methfessel–Paxton smearing<sup>42</sup> of 0.1 eV.

All surfaces are modeled with a four-layer slab and a symmetric adsorption on both sides of the slab, including a relaxation of the uppermost layer. For the geometry relaxation, a criterion of 0.02 eV/Å on forces is used. For the adsorption of 1,3-butadiene and 1-butene, the molecules have been adsorbed on only one side of the substrate. In this case, energy corrections have been applied as implemented in VASP within the spirit of refs 43 and 44 by taking account of the resulting dipole moment energy between the two surfaces of the slab.

The vibrational analysis has been performed within a harmonic approach, using atomic displacements of 0.005 Å in the three directions of space for the adsorbate and neglecting the coupling with the substrate. We calculate the dipole activity of a given vibrational mode as being proportional to the square of the dipole moment variation with respect to the surface normal for the corresponding mode. This value can be related to the intensity observed in HREEL spectra.

For the electronic analysis, we calculated the change in the work function,  $\Delta\Phi$  (i.e., the difference between the work function of the clean surface and that of the surface covered with the adsorbate). Because this change is related to the dipole moment induced through the adsorption and therefore to the charge redistribution induced through the adsorption, an interpretation with respect to donation and back-donation effects is proposed. Negative values imply stronger donation effects of the molecule and less pronounced back-donation effects, whereas positive values imply more pronounced back-donation and fewer donation effects.

Section 4 proposes an approach to take into account the thermal contributions as a function of temperature and pressure. For that purpose, we must calculate the Gibbs free energy of adsorption, which is defined as follows:

$$\Delta G = G_{\text{ads}} - G_{\text{gas}} - G_{\text{surf}} \quad (1)$$

where  $G_{\text{ads}}$ ,  $G_{\text{gas}}$ , and  $G_{\text{surf}}$  stand for the Gibbs free energy of the three systems: the adsorbed molecule, the molecule in the gas phase, and the surface alone, respectively. According to ref 45,  $G$  can be written as

$$G = -NkT \ln\left(\frac{Z}{N}\right) - NkT + pV \quad (2)$$

where  $Z$  is the one-particle partition function of indistinguishable particles.

Neglecting the variation of the  $pV$  terms during adsorption and assuming decoupling between the surface and adsorbate, we can deduce that

$$\Delta G \approx N \left[ E_{\text{ads}} - kT \ln\left(\frac{Z_{\text{ads}}}{Z_{\text{gas}}}\right) \right] \quad (3)$$

where  $E_{\text{ads}}$  stands for the adsorption energy expressed in eV per molecule.  $E_{\text{ads}}$  is calculated at a given coverage,  $\Theta$ , (i.e., the number of adsorbed molecules per surface atom) from the difference in the total electronic energies of the three systems at 0 K without ZPE contributions.

We can finally normalize  $\Delta G$  in eV per surface unit by dividing  $N$  by the number of corresponding surface atoms used for the calculation:

$$\Delta G(T, P) = \Theta \left[ E_{\text{ads}} - kT \ln\left(\frac{Z_{\text{ads}}}{Z_{\text{gas}}}\right) \right] \quad (4)$$

Hence, eq 4 allows us to determine the stability of the adsorbates at the surface as a function of  $T$  and  $P$ . For given values of the temperature  $T$  and the pressure  $P$ , the favored surface coverage  $\Theta$  is the one leading to the minimum value of  $\Delta G$ . In the case of a predominantly repulsive adsorbate–adsorbate interaction, an increasing temperature (decreasing pressure) therefore induces a decrease in  $\Theta$  at a fixed pressure (fixed temperature) (i.e., a desorption of a certain number of molecules).

$Z_{\text{ads}}$  ( $Z_{\text{gas}}$ ) stands for the partition function of the molecule in the adsorbed state (gas phase) including the vibrational, rotational, and translational contributions. For the gas-phase molecule, it consists of

$$Z_{\text{gas}} = Z_{\text{gas}}(\text{rot}) Z_{\text{gas}}(\text{trans}) Z_{\text{gas}}(\text{vib}) \quad (5)$$

For the adsorbed case, the translational and rotational contributions are transformed in additional vibrational contributions (i.e.  $Z_{\text{ads}} = Z_{\text{gas}}(\text{vib})$ ). Additional approximations are made in the evaluation of the partition function. The rotational partition function is evaluated classically because the quantum effects are negligible for the rotational description of the investigated molecules. In addition, the marginal difference between the zero-point corrections (ZPE) for the free molecule and the adsorbed state allows us to neglect the ZPE for this approach. Finally, the vibrational partition functions of the adsorbed molecule and the molecule in the gas phase are assumed to be of a similar value and therefore cancel out, implying that

$$\frac{Z_{\text{ads}}}{Z_{\text{gas}}} = \frac{Z_{\text{ads}}(\text{vib})}{[Z_{\text{gas}}(\text{vib}) Z_{\text{gas}}(\text{rot}) Z_{\text{gas}}(\text{trans})]} \approx \frac{1}{[Z_{\text{gas}}(\text{rot}) Z_{\text{gas}}(\text{trans})]} \quad (6)$$

Although this approximation might seem crude, several tests have shown that it is justified for temperature conditions in which the vibrational partition function is nearly frozen. For the adsorption of 1,3-butadiene on Pt(111) at a coverage of  $1/7$  ML and a temperature of 300 K, a difference of only  $\Delta G(\text{vib}) = 0.007$  eV/surface atom independent of the pressure (corresponding to an underestimation of the desorption temperature of about 20 K at a pressure of  $10^{-9}$  bar) is found between this approach and a approach including the evaluation of the vibrational partition function. Although the absolute values given by this approach should be handled with care, such a model

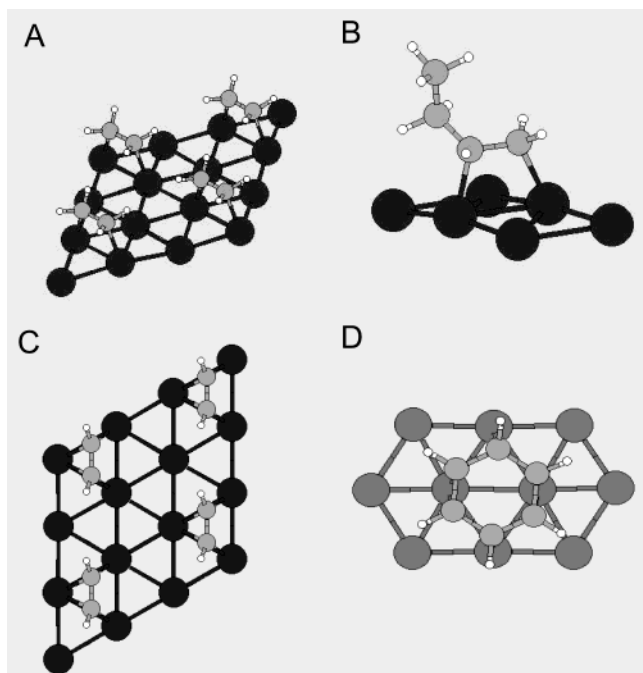


**Figure 1.** Energetically favored adsorption configurations on Pd(111) or Pt(111): (A) ethylene in a di- $\sigma$  mode for the  $p(2 \times 2)$  superstructure, (B) 1-butene in a di- $\sigma$  mode for the  $p(2 \times 2)$  superstructure, (C) acetylene in 3-fold hollow sites for the  $p(2 \times 2)$  superstructure, and (D) benzene in a flat mode above bridge sites for the  $(\sqrt{7} \times \sqrt{7})R19^\circ$  superstructure.

allows a semiquantitative description pointing out the general concepts in adsorption.

### 3. Adsorption of Hydrocarbons on Pt(111) and Pd(111)

**3.1. Adsorption of Olefins.** *3.1.1 Case of Ethylene.* The hydrogenation of ethylene is often seen as a classical model for the hydrogenation of olefins; therefore, a vast number of experimental and theoretical studies have investigated this system.<sup>3–10</sup> For this reason, we will only briefly mention the relevant results. In agreement with the experimentally observed structure,<sup>4</sup> the calculations were performed with ethylene forming a  $p(2 \times 2)$  superstructure. Although EELS spectra might indicate an occupation of both  $\pi$  and di- $\sigma$  type positions, we find in agreement with other theoretical investigations<sup>5,13</sup> that the di- $\sigma$  type adsorption, as illustrated in Figure 1A, is energetically favored for both metals.

The adsorption energy for ethylene on Pt(111) in the di- $\sigma$  mode,  $E_{\text{ads}} = -1.10$  eV, is significantly higher than on Pd(111) with a value of  $E_{\text{ads}} = -0.87$  eV. In both cases, the molecule adsorbs with the double bond parallel to the surface. The interaction results in a stretching of the C=C double bond, which is more pronounced in the case of Pt ( $d(\text{C}=\text{C}) = 1.49$  Å) than for the Pd surface ( $d(\text{C}=\text{C}) = 1.45$  Å). Consequently, the corresponding C=C stretching mode is shifted to a value of  $1042\text{ cm}^{-1}$  (experimentally,  $1060\text{ cm}^{-1}$ )<sup>9</sup> for the adsorption on the Pt surface.

The work function is decreased by a value of  $\Delta\Phi = -1.51$  eV for Pt(111) and  $\Delta\Phi = -1.16$  eV for Pd(111) with respect to the clean surface. The negative value of  $\Delta\Phi$  indicates that the adsorption is dominated by donation rather than back-donation effects. Additional insight into the electronic properties can be gained from an analysis of the density of states (DOS) of the adsorbate (Figure 2). This projection is directly accessible within the PAW formalism of VASP.<sup>38,39</sup> In a simple frontier orbital model, the interaction would be expected to take place

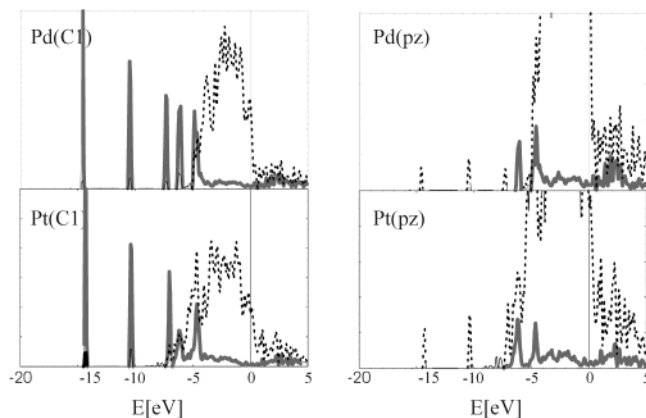


**Figure 2.** Density of states of ethylene adsorbed on Pt(111) and Pd(111) projected onto one of the carbon atoms (left side) and further onto the carbon  $p_z$  states (right side). Dashed lines are for the metal d states, and thick lines are for the carbon states.

via the interaction of the HOMO and the LUMO, both molecular  $\pi$  states, with the surface.

Indeed, the projection of the DOS onto the  $p_z$  states of one carbon atom shows a strong mixing of these states with the metal d band. In the case of the adsorption on Pd(111), the main peaks for the bonding and antibonding  $\pi$  orbitals can be found at binding energies of  $-4.6$  and  $1.84$  eV with respect to the Fermi level, corresponding to a chemical shift of  $2.3$  eV for the HOMO and  $1.6$  eV for the LUMO. Antibonding hybrid states are found filled at binding energies of  $-2.7$  and  $-1.31$  eV. Although the structural parameters of the Pd(111) and the Pt(111) surfaces are rather similar, the comparison between the different substrates illustrates the difference in the electronic properties. In the case of the adsorption on the Pt(111) surface, a significantly stronger orbital mixing with the substrate is observed mainly because of the broader d band of Pt.

*3.1.2. Case of 1-Butene.* In contrast to the situation for ethylene, only a few experimental data are available for the adsorption of the second type of olefin considered in this work, 1-butene. An early EELS study by Avery et al.<sup>46</sup> indicates that 1-butene is adsorbed on Pt(111) in a di- $\sigma$  mode at temperatures below 200 K. In addition, that same study presents evidence that a rather dehydrogenated form, a  $\text{C}_4\text{H}_7$  butylidyne species, is observed at a temperature of 300 K under UHV conditions. NEXAFS experiments performed by Bertolini and co-workers<sup>31</sup> for the adsorption of 1-butene on Pd(111) and Pt(111) confirm the di- $\sigma$  adsorption for Pt(111). However, they observe a narrower  $\pi^*$  resonance for the adsorption on Pd(111), from which they conclude that the molecule would be adsorbed undistorted and presumably in a  $\pi$  mode.

From a theoretical point of view, the chemical similarity between ethylene and 1-butene allows us to expect comparable adsorption on the two surfaces, that is, the adsorption in a di- $\sigma$  mode as illustrated in Figure 1B. Because of the extended size of the molecule, the adsorption has been investigated for two coverages: in a  $p(2 \times 2)$  phase (i.e., a coverage of  $\Theta = 0.25$  ML) corresponding to the superstructure of ethylene and a lower-coverage  $(\sqrt{7} \times \sqrt{7})R19^\circ$  superstructure ( $\Theta = 0.14$  ML). The structural parameters are independent of the coverage, in a similar way as for the adsorption of ethylene. The C=C double bond is stretched to  $1.45$  Å on the Pd(111) surface and to  $1.49$  Å on Pt(111). However, the adsorption energies are comparatively strongly reduced. For the adsorption in the  $p(2 \times 2)$  structure ( $\Theta = 0.25$  ML), we find an adsorption energy of  $E_{\text{ads}} = -0.75$  eV for the Pt(111) surface and  $E_{\text{ads}} = -0.52$  eV for



the Pd(111) surface. In the lower-coverage case ( $\Theta = 0.14$  ML), the adsorption energies decrease to  $E_{\text{ads}} = -0.82$  and  $-0.68$  eV, respectively. This indicates clearly that the reduced adsorption energy in comparison to ethylene is not due to only the stronger adsorbate–adsorbate repulsion of the larger molecules. The explanation can be found in the fact that the 1-butene molecule is strongly distorted, including a change from  $sp^2$  to a  $sp^3$  hybridization of the C2. The separation into the energy contributions relevant for the adsorption of  $p(2 \times 2)$  ethylene and  $(\sqrt{7} \times \sqrt{7})R19^\circ$  1-butene on Pt(111) shows that the deformation energy of ethylene is about  $\Delta E_{\text{deform}}(\text{C}_2\text{H}_4) = 1.43$  eV, to be compared to  $\Delta E_{\text{deform}}(\text{C}_4\text{H}_8) = 1.52$  eV, and that the surface deformation energy is  $\Delta E_{\text{deform}}(\text{surf}) = 0.11$  eV upon ethylene adsorption and 0.19 eV for butene adsorption. Because we find a similar energy gain through the interaction of the double bond with the surface, the higher energetic cost for the deformation of the molecule as well as the surface explains the decrease in the total adsorption energy in the case of 1-butene.

**3.2. Adsorption of Acetylene.** The adsorption of acetylene on Pt(111) and Pd(111) surfaces has been investigated in a large number of experimental<sup>8,14,16,17</sup> and theoretical<sup>11,18,19</sup> studies. It has been established as well from a LEED study<sup>14</sup> and from STM experiments<sup>16</sup> that the molecule adsorbs on the Pd(111) surfaces both in  $(2 \times 2)$  and  $(\sqrt{3} \times \sqrt{3})$  superstructures. For computational reasons, we restricted our work to the investigation of the  $p(2 \times 2)$  phase.

In agreement with other recent DFT studies,<sup>11,18</sup> we find an adsorption in a hollow position with adsorption energies of 2.26 eV on Pt(111) and 2.03 eV on Pd(111) as the energetically preferred adsorption mode for both surfaces. Figure 1C illustrates the adsorption position on both metals: the C≡C bond is elongated to 1.37 Å on Pd and 1.40 Å on Pt, resulting in C–M distances of 2.18 Å/2.01 Å (Pd) and 2.20 Å/2.01 Å (Pt). Upon adsorption, the work function of the surface is decreased by  $\Delta\Phi = -1.31$  eV on Pd and  $\Delta\Phi = -1.77$  eV on Pt. According to these values, we deduce that the charge transfer from the molecule to the bond and the surface is more pronounced for the adsorption of acetylene than for ethylene.

**3.3. Adsorption of Benzene.** The adsorption of benzene on Pd(111) and Pt(111) surfaces is often seen as a representative system for the interaction of aromatic molecules with catalytically relevant metal surfaces and has therefore been investigated in a vast number of experimental<sup>8,17,21–26</sup> and theoretical<sup>27–29</sup> studies. We investigated the adsorption in a  $(\sqrt{7} \times \sqrt{7})R19^\circ$  superstructure resulting in a coverage of  $\Theta = 0.14$  ML.

The calculated adsorption energies with values of  $-0.85$  eV on Pt(111) and  $-1.04$  eV on Pd(111) are slightly lower than the values reported by Morin et al.<sup>29</sup> obtained at a lower coverage. However, the results confirm their observations: the energetically favored adsorption mode on both surfaces is an adsorption in the bridge site with the aromatic ring parallel to the surface (Figure 1D). In comparison with the other adsorbates, benzene is the only molecule for which we find a higher adsorption energy for the Pd surface than for the Pt surface. Because of the loss of aromaticity, the C–C distances are stretched to values of 1.43/1.45 Å on Pd and 1.43/1.47 Å on Pt. The adsorption induces a reduction of the work function by  $\Delta\Phi = -1.72$  eV on Pd and  $\Delta\Phi = -2.32$  eV on Pt. As for ethylene and acetylene, these values underline the predominant donating character of the interaction of benzene with these Pd and Pt surfaces.

**3.4. Adsorption of 1,3-Butadiene.** When submitting this paper, a similar study<sup>47</sup> on the adsorption of 1,3-butadiene and butenes on Pd(111) and Pt(111) was brought to our knowledge.

Although the adsorption of ethylene or acetylene is covered by a vast amount of experimental data, the adsorption of 1,3-butadiene on Pt(111) and Pd(111) has been the subject of fewer investigations in the theoretical literature. However, it represents one of the challenges toward an understanding of the selective hydrogenation of diolefins. An early EELS study<sup>30</sup> for butadiene over Pt(111) suggested an  $\eta 2$  di- $\sigma$  adsorption for low temperatures (170 K) and a tetra- $\sigma$  adsorption for 300 K. Bertolini and co-workers have investigated the adsorption on Pd(111) and Pt(111) with a combined NEXAFS and HREELS study<sup>31</sup> in which they found only a loose adsorption at 95 K. At a temperature of 300 K, they found an adsorption parallel to the surface. In addition, they observed a discernible  $\pi^*_1 - \pi^*_2$  splitting for the adsorption on the Pd(111) surface, in contrast to only one broad  $\pi^*$  peak for the Pt surface. These observations were attributed to a di- $\pi$  adsorption on the Pd surface and a  $\sigma$  adsorption on the Pt surface. Sautet and Paul<sup>6</sup> compared two adsorption configurations ( $\eta 2$  di- $\sigma$  and  $\eta 4$  di- $\pi$ ) with the help of extended Hückel calculations applied to cluster models. They proposed that for both Pd(111) and Pt(111) the  $\eta 4$  adsorption is preferred. However, at that time it was not possible to determine rigorously the energetically stable adsorbed states. Thus, in contrast to most of the other adsorbates, this adsorption has not been covered by state-of-the-art DFT investigations; therefore, we propose, in what follows, a detailed analysis of the adsorption configurations.

The complexity of the molecule allows for a large number of adsorption configurations, and the relative energetic order is influenced by the coverage. Figure 3 gives an overview over the main relevant adsorption configurations. The following notations for the adsorption configurations are classified according to the type of adsorbed isomer (trans and cis), the number of carbon atoms interacting with the surface ( $\eta 1 - \eta 4$ ), and the type of chemical bonding ( $\sigma$  and  $\pi$ ). Although additional configurations have been investigated, notably an adsorption configuration of the  $\eta 3$  type, we report only the most stable ones.

Table 1 (Table 2) gives an account for the adsorption energies obtained for Pt(111) (Pd(111)) as a function of the coverage. From a general point of view, butadiene exhibits stronger adsorption energies on Pt than on Pd, as already observed for ethylene and acetylene. At the highest coverage ( $\Theta = 0.33$  ML), the adsorption in only the  $\eta 2$  configuration has been considered because of steric reasons. For both surfaces, the adsorption energy is strongly reduced when compared to the same position at lower coverages. For  $\Theta = 0.25$  ML represented by the  $p(2 \times 2)$  structure, we find for both surfaces a competition between the  $\eta 2$  and the  $\eta 4$  configurations.

For Pt, the competing configurations are the  $\eta 2$  and the  $\eta 4$  di- $\sigma/\pi$  (E) with adsorption energies of  $-0.69$  and  $-0.71$  eV, respectively. For Pd, the  $\eta 2$  configuration is also competing with the  $\eta 4$  configurations with adsorption energies ranging from  $-0.53$  to  $-0.60$  eV. At this stage, it is also interesting that the trans  $\eta 4$  and  $\eta 2$  configurations are more strongly destabilized on Pd than on Pt. This effect is particularly pronounced for the trans  $\eta 4$  tetra- $\sigma$  configuration, which is due to the smaller Pd–Pd distance, implying stronger intermolecular repulsive interactions within the  $p(2 \times 2)$  structure. However, if the molecules are rearranged in a  $c(4 \times 2)$  superstructure resulting in the same coverage of 0.25 ML, we find a preferred  $\eta 4$  tetra- $\sigma$ -like adsorption configuration, resulting in adsorption energies of  $E_{\text{ads}} = -1.09$  eV for Pt and  $E_{\text{ads}} = -0.79$  eV for Pd. This superstructure allows a significant reduction of the repulsive lateral interactions. For both surfaces, the low-coverage limit

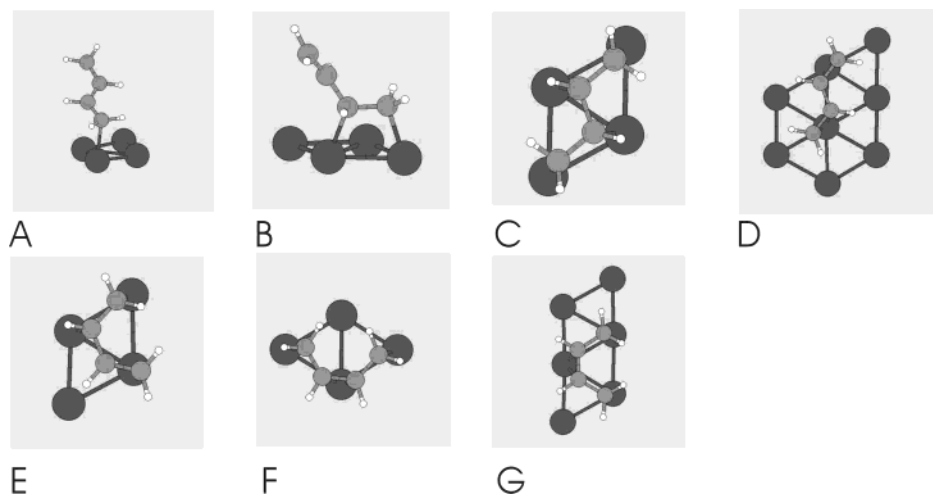


**Figure 3.** Adsorption configurations of 1,3-butadiene: (A) trans  $\eta 1$ , (B) trans  $\eta 2$ , (C) trans  $\eta 4$  tetra- $\sigma$ , (D) trans  $\eta 4$  di- $\pi$ , (E) cis  $\eta 4$  di- $\sigma/\pi$ , (F) cis  $\eta 4$  di- $\sigma/\pi$ , (G) cis  $\eta 4$  di- $\sigma/\pi$ .

**TABLE 1: Adsorption Energies (in eV/molecule) for 1,3-Butadiene on Pt(111)**

	$\sqrt{3} \times \sqrt{3}$ ( $\Theta = 0.33$ ML)	$p(2 \times 2)$ ( $\Theta = 0.25$ ML)	$c(4 \times 2)$ ( $\Theta = 0.25$ ML)	$p(2 \times 3)$ ( $\Theta = 0.17$ ML)	$(\sqrt{7} \times \sqrt{7})R19^\circ$ ( $\Theta = 0.14$ ML)	$p(3 \times 3)$ ( $\Theta = 0.11$ ML)
trans $\eta 1$ (A)		-0.07				
trans $\eta 2$ (B)	-0.34	-0.69			-0.78	
trans $\eta 4$ tetra- $\sigma$ (C)		-0.61	-1.09	-1.48	-1.55	-1.58
trans $\eta 4$ di- $\pi$ (D)					-0.99	
cis $\eta 4$ di- $\sigma/\pi$ (E)		-0.71	-0.69	-1.22	-1.28	
cis $\eta 4$ di- $\sigma/\pi$ (F)		-0.61	-	-	-	
cis $\eta 4$ di- $\sigma/\pi$ (G)		-0.63	-	-1.29	-	

**TABLE 2: Adsorption Energies (in eV/molecule) for the Adsorption of 1,3-Butadiene on Pd(111)**

	$\sqrt{3} \times \sqrt{3}$ ( $\Theta = 0.33$ ML)	$p(2 \times 2)$ ( $\Theta = 0.25$ ML)	$c(4 \times 2)$ ( $\Theta = 0.25$ ML)	$p(2 \times 3)$ ( $\Theta = 0.17$ ML)	$(\sqrt{7} \times \sqrt{7})R19^\circ$ ( $\Theta = 0.14$ ML)	$p(3 \times 3)$ ( $\Theta = 0.11$ ML)
trans $\eta 2$ (B)		-0.53			-0.75	
trans $\eta 4$ tetra- $\sigma$ (C)	-0.15	-0.28	-0.79	-1.37	-1.43	-1.48
trans $\eta 4$ di- $\pi$ (D)					-1.17	
cis $\eta 4$ di- $\sigma/\pi$ (E)		-0.60	-0.62		-1.00	
cis $\eta 4$ di- $\sigma/\pi$ (F)		-0.56				
cis $\eta 4$ di- $\sigma/\pi$ (G)				-1.22		

**TABLE 3: Selected Vibrational Modes (in cm<sup>-1</sup>) of 1,3-Butadiene on Pt(111)**

	C <sub>4</sub> H <sub>6</sub> : gas (calc.)	C <sub>4</sub> H <sub>6</sub> /Pt: p(2X2) trans $\eta 2$ (A)	C <sub>4</sub> H <sub>6</sub> /Pt: p(3X2) trans $\eta 4$ di- $\sigma/\pi$ (G)	C <sub>4</sub> H <sub>6</sub> /Pt: ( $\sqrt{7} \times \sqrt{7}$ ) trans $\eta 4$ quadri- $\sigma$ (C)	C <sub>4</sub> H <sub>6</sub> /Pt expt <sup>31</sup>
$\nu(\text{CH}_2)$		3165			
antisym	3175/3176	3079/3094	3122/3100	3099/3090	
sym	3087/3084	3009	3085/3079	3001/2997	2990
$\nu(\text{CH})$	3081	2986/3009	2998/3011	2990/2994	2895
	3069				
$\nu(\text{C}=\text{C})$	1647				
	1599	1598	1415	1228/1338	1430
$\delta(\text{CH}_2)$	1431	1409	1436/1406	1415/1409	
	1376				

is reached in the  $p(2 \times 3)$  phase, a further reduction of the coverage results in only a slight energy gain of less than 0.1 eV for Pt and Pd without modifying the energetically favored adsorption  $\eta 4$  tetra- $\sigma$  configuration or the corresponding elongation of the two C=C bonds to uniform values of 1.44 Å (Pd) and 1.48 Å (Pt).

Additional insight into the adsorption configuration can be gained from the analysis of the vibrational properties of the

adsorbates, as reported in Tables 3 and 4. The vibrational frequencies have been determined within a harmonic approach; therefore, the C–H stretching frequencies are overestimated by about 80 to 100 cm<sup>-1</sup> (when compared with the gas phase). In addition, one should keep in mind that the symmetry of the adsorbate is further reduced in comparison to that of the gas-phase molecule; therefore, a precise assignment of the vibrational modes to their gas-phase equivalent is not always possible.

TABLE 4: Selected Vibrational Modes of 1,3-Butadiene on Pd(111)

	C <sub>4</sub> H <sub>6</sub> : (gas)	C <sub>4</sub> H <sub>6</sub> /Pd: ( $\sqrt{7}\times\sqrt{7}$ )	C <sub>4</sub> H <sub>6</sub> /Pd: ( $\sqrt{7}\times\sqrt{7}$ )	C <sub>4</sub> H <sub>6</sub> /Pd: ( $\sqrt{7}\times\sqrt{7}$ )
	(calc)	trans $\eta 2$ (A)	trans $\eta 4$ tetra- $\sigma$ (C)	trans $\eta 4$ di- $\pi$ (D)
$\nu(\text{CH}_2)$		3172		3166/3163
antisym	3175/3176	3087/3085	3097/3098	3078/3077
sym	3087/3084	3078	3009/3010	3076
$\nu(\text{CH})$	3081	3032	2884/2992	3038
	3069	2999		
$\nu(\text{C}=\text{C})$	1647			
	1599	1579	1438	1498
$\delta(\text{CH}_2)$	1431	1427	1413	1448
	1376			

For instance, this explains why for the CH<sub>2</sub> groups we find a higher number of modes than in the gas phase. Nevertheless, we find a similar trend for both surfaces: if butadiene is adsorbed in the energetically favored  $\eta 4$  tetra- $\sigma$  configuration then both groups corresponding to the CH stretching mode at about 3175 and 3080 cm<sup>-1</sup> are shifted by 80 cm<sup>-1</sup> to lower wavenumbers. In addition, the loss of the double bonds is reflected in the decrease of the frequency of the corresponding modes (gas-phase value: 1647 and 1599 cm<sup>-1</sup>). In contrast, adsorption in the  $\eta 2$  configuration would lead on both surfaces to a significantly different spectrum because the stretching frequency  $\nu(\text{CH}_2)$  of the methyl group tilted away from the surface (3165 cm<sup>-1</sup> for Pt(111), and 3172 cm<sup>-1</sup> for Pd(111)) would remain close to the calculated gas-phase value of 3175 cm<sup>-1</sup>. Furthermore, whereas all C=C bonds would be stretched to uniform values of 1.48 Å (Pt) and 1.45 Å (Pd) in the case of an  $\eta 4$ -trans adsorption, one of the double bonds is kept at 1.34 Å on both surfaces for the  $\eta 2$  configuration. This double bond would correspond to a vibrational mode at frequencies of 1598 cm<sup>-1</sup> (Pt) and 1579 cm<sup>-1</sup> (Pd).

The simulation of the dipole activity of the mode located at 1598 cm<sup>-1</sup> for Pt(111) shows that it is dependent on the coverage. At a high coverage  $p(2 \times 2)$ , where a stronger tilting of the C3=C4 double bond is produced, the peak is visible (see asterisk in Figure 4). However, it is nearly suppressed at lower

coverages. For the high-frequency region, the simulated spectra show that two peaks can be distinguished around 3000 and 3100 cm<sup>-1</sup>. In the  $\eta 4$  configuration, the highest intensity is obtained at 3000 cm<sup>-1</sup>, which is compatible with observations made in ref 31. Furthermore, the simulated spectra also reveal that a clear differentiation can be obtained via carbon-carbon modes found in the region of 650–1000 cm<sup>-1</sup> because two modes with values of 758 and 898 cm<sup>-1</sup> are predicted for the adsorption in the  $\eta 4$  tetra- $\sigma$  configuration, whereas the  $\eta 2$  adsorption would result in visible modes at 658, 857, and 882 cm<sup>-1</sup>. Because the experimentally observed modes<sup>31</sup> are found at values of 760 and 890 cm<sup>-1</sup>, adsorption in the  $\eta 2$  configuration can be ruled out for Pt(111).

The adsorption in the  $\eta 4$  di- $\sigma/\pi$  cis (G) configuration, energetically disfavored by 0.15–0.19 eV for low coverages, results in one stronger C2–C3 bond with a  $\pi$ -type interaction. Consequently, the corresponding frequency for this bond (1415 cm<sup>-1</sup>) is higher than in the  $\eta 4$  tetra- $\sigma$  configuration, and also the highest (infrared active) C2(C3)–H stretching modes are shifted only to 3122 cm<sup>-1</sup>. Yet, because the resulting vibrational spectra of those two adsorption configurations are quite similar, the distinction between these two configurations based on HREELS characterization cannot be solved without ambiguity.

Finally, Table 4 also reports results for the  $\eta 4$  di- $\pi$  trans (D) configuration on Pd, revealing that it would not be compatible with HREELS results according to the  $\nu(\text{CH}_2)$  frequencies remaining too close to the gas-phase values.

An analysis of the density of states of 1,3-butadiene adsorbed in a ( $\sqrt{7} \times \sqrt{7}$ )R19° superstructure in the favored  $\eta 4$  tetra- $\sigma$  configuration illustrates again an interaction of the bonding  $\pi$  states as well as the antibonding  $\pi^*$  states with the metal d band (Figure 5). As in the case of the adsorption of the other hydrocarbons, we find stronger orbital mixing between the substrate and the adsorbate as well as a more pronounced elongation of the C=C bonds in the case of the adsorption on the Pt(111) surface compared to that on the Pd(111) surface. This difference is also reflected in the hybridization state of the antibonding  $\pi^*$  states. Whereas two discernible peaks (see arrows on Figure 5) are found at binding energies of -2.8 and -1.1 eV below the Fermi level and at 1.8 and 3 eV above the Fermi level for the adsorption on the Pd surface, the identification of the corresponding states for the adsorption on the Pt surface is rather difficult due to the broadening of the states. This difference could offer an explanation for the observed

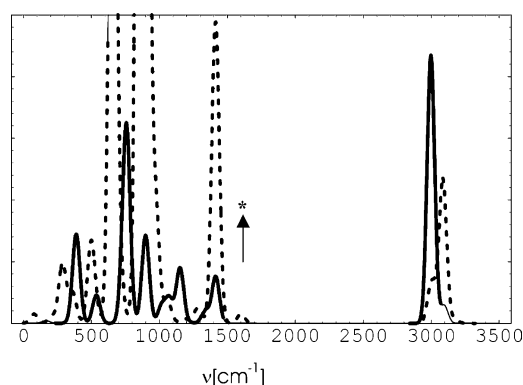


**Figure 4.** Simulated vibrational spectrum for the adsorption of ( $\sqrt{7} \times \sqrt{7}$ )R19° butadiene on Pd(111) in the trans  $\eta 4$  tetra- $\sigma$  configuration (solid line) and the  $\eta 2$  configuration (dashed line). The asterisk indicates the simulated intensity of the mode at 1598 cm<sup>-1</sup> for the  $\eta 2$  configuration in the  $p(2 \times 2)$  superstructure (same scaling as for the ( $\sqrt{7} \times \sqrt{7}$ )  $\eta 2$  configuration).

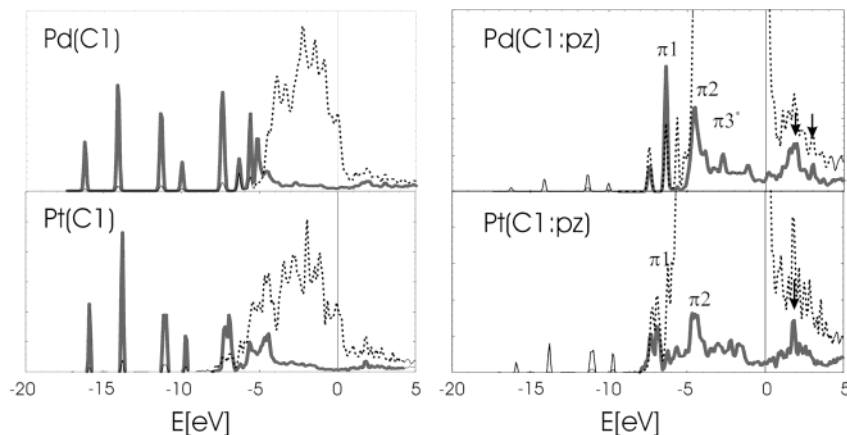


**Figure 5.** Density of states for 1,3-butadiene on Pd(111) and Pt(111) projected onto the first carbon atom (left) and onto the carbon  $p_z$  states (right). Dashed lines are for the metal d states, and thick lines are for the carbon states.

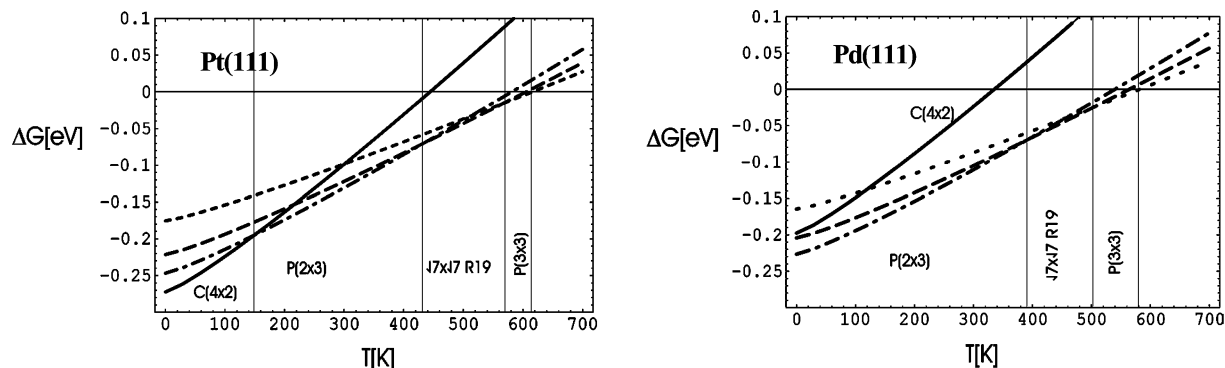


**Figure 6.** Relative Gibbs energy for the adsorption of 1,3-butadiene at a pressure of 1 bar on Pt(111) (left) and Pd(111) (right).

**TABLE 5: Adsorption Energies (in eV/surface atom) Corresponding to the Value of  $\Theta \cdot E_{\text{ads}}$  in Equation 1 for Hydrocarbons Adsorbed on Pd(111) and on Pt(111)**

	acetylene p(2 × 2)	1,3-butadiene Pt: c(4 × 2), Pd: p(2 × 3)	ethylene p(2 × 2)	1-butene p(2 × 2)	benzene ( $\sqrt{7} \times \sqrt{7}$ )R19°
Pd(111)	-0.488	-0.227	-0.218	-0.130	-0.149
Pt(111)	-0.545	-0.273	-0.275	-0.187	-0.121

NEXAFS spectra,<sup>31</sup> revealing two distinct peaks at the C-edge separated by 1.5 eV for the adsorption on Pd(111), in contrast to one single peak on Pt(111).

#### 4. Effects of Temperature and Pressure

The data obtained in section 3 on adsorption allow us to establish a classification of the molecules. The most basic approach would be the comparison of the adsorption energies for the favored superstructures and adsorption configurations rescaled by the respective coverages, which would correspond to the adsorption behavior in the low-temperature limit (Table 5). We find that, with the exception of benzene, the adsorption on Pt(111) results generally in higher adsorption energies. The trends between the adsorbates are roughly the same for both surfaces: the strongest adsorption is found for acetylene, a comparable and intermediate value is found for the adsorption of ethylene and butadiene, and the weakest adsorption is found for butene and for benzene.

However, the thermal contributions cannot be neglected for higher temperatures and pressures. Hence, we apply the approach proposed in section 2 to investigate these effects induced by the term  $-\Theta kT \ln(Z_{\text{ads}}/Z_{\text{gas}})$  of eq 1. For the adsorption of 1,3-butadiene on Pt(111), a comparison between the different coverages shows that in the low-temperature limit and at a given

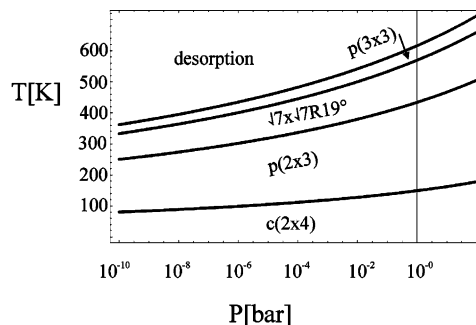


**Figure 7.** Phase diagram of the different stable superstructures of butadiene on the Pt(111) surface as a function of pressure and temperature.

pressure of 1 bar the c(4 × 2) superstructure ( $\Theta = 0.25$  ML) is the most stable phase (Figure 6). At a temperature of about 150 K, the favored phase corresponds to a lower coverage of 0.17 ML, represented by the p(2 × 3) superstructure. Upon further increases of temperature, the ( $\sqrt{7} \times \sqrt{7}$ )R19° superstructure ( $\Theta = 0.14$  ML) and the p(3 × 3) superstructure ( $\Theta = 0.11$  ML) are stabilized. Above  $T_{\text{des}} = 620$  K, no molecule remains on the surface. The adsorption on the Pd(111) surface (Figure 6) occurs in a similar way, although the lower adsorption energies result in slightly lower desorption temperatures; in particular, above  $T_{\text{des}} = 580$  K, all molecules are desorbed. In addition, the weaker Gibbs adsorption energy for the c(4 × 2) phase prevents the existence of this superstructure; therefore, the low-temperature regime is dominated by an adsorption in the p(2 × 3) phase.

With increasing pressure (Figure 7), each transition temperature including the desorption temperature is shifted toward higher temperatures; therefore, the temperature regime for each



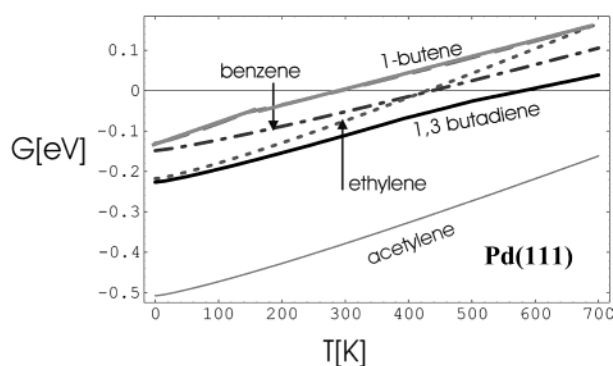
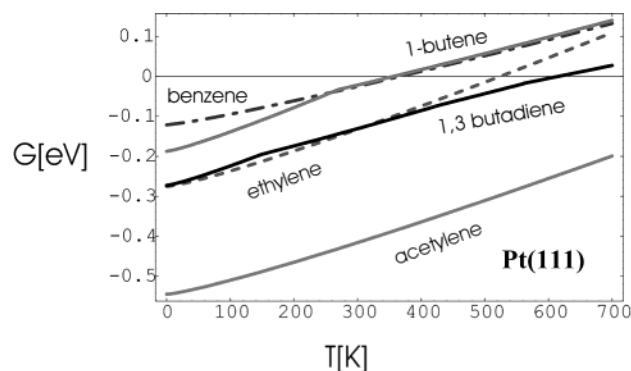


**Figure 8.** Relative Gibbs energy of benzene, ethylene, 1,3-butadiene, 1-butene, and acetylene adsorbed on Pt(111) (left) and Pd(111) (right) at  $P = 1$  bar.

**TABLE 6: Comparison of  $\Delta G$  (in eV per surface atom) for the Adsorption of Hydrocarbons on Pt(111) and Pd(111) at  $T = 300$  K and  $P = 1$  bar**

	acetylene	1,3-butadiene p(2 × 3)	ethylene	benzene	1-butene ( $\sqrt{7} \times \sqrt{7}$ )R19°
Pd(111)	-0.358	-0.111	-0.075	-0.052	0.002
Pt(111)	-0.416	-0.131	-0.132	-0.025	-0.019

stable phase is expanded. Nevertheless, the order of the phases will remain the same.

Figure 8 illustrates the quantitative comparison of the Gibbs free adsorption energy for the five simulated molecules adsorbed on Pt and on Pd at a partial pressure of 1 bar. For butadiene and 1-butene, the most stable coverages are reported for each temperature regime (i.e., the lowest value in  $\Delta G$ ), which explains why piecewise linear plots are appearing.

First, this Figure illustrates that acetylene is the most strongly adsorbed species on Pd and Pt, whatever the temperature may be. Even at high (but realistic) partial pressures of the other species, acetylene remains the most strongly adsorbed molecule on the surface. As a consequence, this explains why a small concentration of alkynes could poison the metallic surface very easily, regarding the hydrogenation of hydrocarbon molecules with lower degrees of unsaturation and regardless of the metallic substrate. This strong inhibiting effect of acetylene has also been evidenced for other reactions such as the oxidation of CO on postcombustion PtRh catalysts.<sup>48</sup> In this case, a very small amount of acetylene may significantly slow the oxidation reaction, whereas this effect is less pronounced for olefins and diolefins.

Benzene and 1-butene are among the weakest adsorbed species at a pressure of 1 bar. However, on Pd(111), where the adsorption of benzene is stronger and the adsorption of ethylene is weaker, a competition takes place between benzene and ethylene close to their desorption temperature. Ethylene and butadiene are located in an intermediate range of Gibbs free energy (Figure 8 and Table 6). We find a competition between ethylene and butadiene on Pt(111), whereas on Pd(111) ethylene is disfavored versus butadiene at all temperatures at the same partial pressure of 1 bar. However, for those two species the competition may depend closely on their relative partial pressures under working conditions.

Finally, we focus more on two relevant species for selective hydrogenation: butadiene and 1-butene. At room temperature and identical partial pressures, it is clear that butadiene is significantly more strongly adsorbed than 1-butene in agreement with kinetic data.<sup>35</sup> So the competition, previously put forward between ethylene and butadiene, no longer takes place between butene and butadiene. This is due to the low adsorption energy of 1-butene.

On Pd as well as on Pt for almost any partial pressure ratio of butene/butadiene, the value of  $\Delta G(\text{butadiene}) - \Delta G(\text{butene})$  remains negative (i.e., in favor of butadiene). This means that during working conditions the surface is mainly covered by the reactants (butadiene and hydrogen) and the products are the minority component on the surface.

It is known experimentally that Pd is more selective toward 1-butene than Pt, the latter yielding a larger amount of butane. At this stage of the study and without any more detailed results on the reaction mechanism, Table 6 shows that the adsorption energy of butadiene is indeed stronger than that of 1-butene; however, there is almost no difference between Pd and Pt regarding the relative adsorption energies of butene versus butadiene. Therefore, we propose that the higher selective hydrogenation on Pd may be due only to the easier desorption of butene from Pd(111) than from Pt(111). According to Table 6, we notice that at room temperature the Gibbs free energy of adsorption of 1-butene is athermal on Pd and the  $\Delta G$  value remains negative on Pt. This implies that at room temperature, as soon as 1-butene is produced, it desorbs on Pd(111), whereas some 1-butene remains adsorbed on the Pt surface, allowing its further transformation to butane on Pt. We suggest that this may be the origin of the higher selectivity in butadiene hydrogenation on Pd(111).

## 5. Conclusions

The adsorption of several unsaturated hydrocarbons on the close-packed Pd(111) and Pt(111) surfaces has been investigated with the help of ab initio calculations. The adsorption of aromatics, as represented by the adsorption of benzene, is dominated by the interaction of the aromatic ring with the surface. The adsorption energy expressed per surface molecule is the lowest.

The adsorption of olefins has been investigated for ethylene and 1-butene. Although both molecules interact with the surface through one double bond, the adsorption energy for 1-butene is significantly lower than that for ethylene on both surfaces. This can not only be explained by the molecular size and the resulting repulsive adsorbate–adsorbate interaction at high coverage but is mainly due to the larger deformation energy of the molecule and surface in the case of 1-butene.

For diolefins adsorption such as that of 1,3-butadiene, the trans  $\eta^4$  tetra- $\sigma$  configuration is energetically favored for Pd(111) and Pd(111) for the relevant coverages at room temperature. The calculated vibrational spectra for the  $\eta^4$  adsorption configuration is compatible with experimental HREELS data, and this analysis allows us to exclude the  $\eta^2$  adsorption



configuration. The cis  $\eta^4$  tetra di- $\pi$  di- $\sigma$  configuration is also compatible with HREELS but appears energetically slightly less favored.

Finally the adsorption of acetylene, representing the interaction of the catalytic surfaces with triple bonds, results in the highest adsorption energy.

For all investigated hydrocarbons, we find a stronger mixing of the molecular  $\pi$  and  $\pi^*$  orbitals with the metal d states for the Pt surface than for the Pd surface. Considering the change in the work function,  $\Delta\Phi$ , we find the following order:

$$0 > \Delta\Phi(\text{benzene}) > \Delta\Phi(\text{acetylene}) > \Delta\Phi(\text{ethylene})$$

with a dominating donation effect on both surfaces.

Using a thermodynamic approach, we show how the thermal stability of adsorbates depends on the pressure and temperature conditions imposed by the working conditions. The adsorption of acetylene remains the strongest, whereas benzene and 1-butene are the most weakly adsorbed species. At typical conditions of 300 K and a pressure of 1 bar, we find the following decreasing order in adsorption stability: acetylene > butadiene  $\approx$  ethylene > benzene  $\approx$  butene on the Pt surface and acetylene > butadiene > ethylene > benzene > butene on the Pd surface. Finally, we suggest that the lower stability of 1-butene on Pd versus Pt may offer a possible explanation for the higher hydrogenation selectivity observed for Pd.

**Acknowledgment.** We are grateful to our colleague Denis Uzio from IFP as well as Philippe Sautet and Françoise Delbecq from ENS Lyon for fruitful discussions. We also thank Andreas Eichler (Universität Wien) for the helpful discussion about the dipole activity of vibrational modes. This work has been undertaken within the GDR 1209 "Dynamique Moléculaire Quantique Appliquée à la Catalyse", a joint project of IFP-CNRS-TOTAL-Universität Wien.

## References and Notes

- (1) Arnold, H.; Döbert, F.; Gaube, J. In *Handbook of Heterogeneous Catalysis*; Ertl, G., Knözinger, H., Weitkamp, J., Eds.; Wiley-VCH: Weinheim, Germany, 1997.
- (2) Cosyns, J. In *Catalyse par les Métaux*; Imelik, B., Martin, G. A., Renouprez, A. J., Eds.; Edition du CNRS: Paris, 1984.
- (3) Sheppard, N.; de la Cruz, C. *Adv. Catal.* **1996**, *41*, 1.
- (4) Yeo, Y. Y.; Stuck, A.; Wartnaby, C. E.; King, D. A. *Chem. Phys. Lett.* **1996**, *259*, 28.
- (5) Ge, Q.; King, D. A. *J. Chem. Phys.* **1999**, *110*, 4699.
- (6) Sautet, P.; Paul, J.-F. *Catal. Lett.* **1991**, *9*, 245.

- (7) Abon, M.; Billy, J.; Bertolini, J. C. *Surf. Sci.* **1986**, L387.
- (8) Tysoe, W. T.; Nyberg, G. L.; Lambert, R. M. *Surf. Sci.* **1983**, *135*, 128.
- (9) Steininger, H.; Ibach, H.; Lehwald, S. *Surf. Sci.* **1982**, *117*, 685.
- (10) Morgan, A. E.; Somorjai, G. A. *J. Chem. Phys.* **1969**, *51*, 3309.
- (11) Sheth, P. A.; Neurock, M.; Smith, C. M. *J. Phys. Chem. B* **2003**, *107*, 2009.
- (12) Neurock, M.; van Santen, R. A. *J. Phys. Chem. B* **2000**, *104*, 11127.
- (13) Pallassana, V.; Neurock, M. *J. Catal.* **2000**, *191*, 301.
- (14) Sandell, A.; Beutler, A.; Jaworowski, A.; Winklund, M.; Heister, K.; Nyholm, R.; Andersen, J. N. *Surf. Sci.* **1998**, *415*, 411.
- (15) Tysoe, W. T.; Nyberg, G. L.; Lambert, R. M. *Surf. Sci.* **1983**, *135*, 128.
- (16) Janssens, T. V. W.; Völkening, S.; Zambelli, T.; Witterlin, J. *J. Phys. Chem. B* **1998**, *102*, 6521.
- (17) Sheppard, N.; de la Cruz, C. *Adv. Catal.* **1998**, *42*, 181.
- (18) Dunphy, J. C.; Rose, M.; Behler, S.; Ogletree, D. F.; Salmeron, M.; Sautet, P. *Phys. Rev. B* **1998**, *57*, R12705.
- (19) Sellers, H. *J. Phys. Chem.* **1990**, *94*, 8329.
- (20) Medlin, J. W.; Allendorf, M. K. *J. Phys. Chem. B* **2003**, *107*, 217.
- (21) Waddill, G. D.; Kesmodel, L. L. *Phys. Rev. B* **1985**, *31*, 4940.
- (22) Waddill, G. D.; Kesmodel, L. L. *Phys. Rev. B* **1985**, *32*, 2107.
- (23) Grassian, V. H.; Muettterties, E. L. *J. Phys. Chem.* **1987**, *91*, 389.
- (24) Xu, C.; Tsai, Y.-L.; Koel, B. E. *J. Phys. Chem.* **1994**, *98*, 585.
- (25) Haq, S.; King, D. A. *J. Phys. Chem.* **1996**, *100*, 16957.
- (26) Wander, A.; Held, G.; Hwang, R. Q.; Blackman, G. S.; Xu, M. L.; de Andres, P.; Van Hove, M. A.; Somorjai, G. A. *Surf. Sci.* **1991**, *249*, 21.
- (27) Lomas, J. R.; Pacchioni, G. *Surf. Sci.* **1996**, *365*, 297.
- (28) Saeys, M.; Reyniers, M.-F.; Marin, G. B.; Neurock, M. *J. Phys. Chem. B* **2002**, *106*, 7489.
- (29) Morin, C.; Simon, D.; Sautet, P. *J. Phys. Chem. B* **2003**, *107*, 2995.
- (30) Avery, N. R.; Sheppard, N. *Proc. R. Soc. London, Ser. A* **1986**, *405*, 27.
- (31) Bertolini, J. C.; Cassuto, A.; Jugnet, Y.; Massardier, J.; Tardy, B.; Tourillon, G. *Surf. Sci.* **1996**, *349*, 88.
- (32) Sautet, P.; Paul, J.-F. *Catal. Lett.* **1991**, *9*, 245.
- (33) Boitiaux, J. P.; Cosyns, J.; Vasudevan, S. *Appl. Catal.* **1983**, *6*, 41.
- (34) Pradier, C.-M.; Margot, E.; Berthier, Y.; Oudar, J. C. *R. Acad. Sci., Ser. II* **1988**, *306*, 561.
- (35) Ouchaib, T.; Massardier, J.; Renouprez, A. *J. Catal.* **1989**, *119*, 517.
- (36) Kresse, G.; Hafner, J. *Phys. Rev. B* **1993**, *47*, C558.
- (37) Kresse, G.; Furthmüller, J. *Comput. Mater. Sci.* **1996**, *6*, 15.
- (38) Blöchl, P. E. *Phys. Rev. B* **1994**, *50*, 17953.
- (39) Kresse, G.; Joubert, D. *Phys. Rev. B* **1999**, *59*, 1758.
- (40) Perdew, J. P.; Chevary, J. A.; Voslo, S. H.; Jackson, K. A.; Pederson, M. R.; Singh, D. J.; Fiolhais, C. *Phys. Rev. B* **1992**, *46*, 6671.
- (41) Monkhorst, H. J.; Pack, J. D. *Phys. Rev. B* **1976**, *13*, 5188.
- (42) Methfessel, M.; Paxton, A. *Phys. Rev. B* **1989**, *40*, 3616.
- (43) Makov, G.; Payne, M. C. *Phys. Rev. B* **1995**, *51*, 4014.
- (44) Neugebauer, J.; Scheffler, M. *Phys. Rev. B* **1992**, *46*, 16067.
- (45) Atkins, P. W. In *Physical Chemistry*, 3rd ed.; W. H. Freeman: New York, 1986.
- (46) Avery, N. R.; Sheppard, N. *Proc. R. Soc. London, Ser. A* **1986**, *405*, 1.
- (47) Valcárcel, A.; Clotet, A.; Ricart, J. M.; Delbecq, F.; Sautet, P. Submitted for publication.
- (48) Mabilon, G.; Durand, D.; Courty, Ph. *Stud. Surf. Sci.* **1995**, *96*, 775.